Radiation hardness of 4*H*-SiC epitaxial layers: The role of deep level defects

Ivana Capan[1,a*], Tomislav Brodar[1,b], Takeshi Ohshima[2,c], Shin-ichiro Sato[2,d], Takahiro Makino[2,e], Željko Pastuović[3,f], Rainer Siegele[3,g], Luka Snoj[4,h], Vladimir Radulović[4,i], José Coutinho[5,j], Vitor J. B. Torres[5,k], Kamel Demmouche[6,l]

[1]Rudjer Boskovic Institute, Bijenicka 54, 10000 Zagreb, Croatia
[2]National Institutes for Quantum and Radiological Science and Technology, 1233 Watanuki, Takasaki, Gunma 370-1292, Japan
[3]Australian Nuclear Science and Technology Organisation, 1New Illawarra Rd, Lucas Heights NSW 2234, Australia
[4]Jožef Stefan Institute, Jamova 39, 1000 Ljubljana, Slovenia
[5]Department of Physics and I3N, University of Aveiro, Campus Santiago, 3810-193 Aveiro, Portugal
[6]Centre Universitaire Ain Temouchent, Institut des Sciences et Technologies, B.P. 284 46000 Ain Temouchent, Algeria

[a]capan©irb.hr, [b]tomislavbrodar@gmail.com, [c]ohshima.takeshi@qst.go.jp, [d]sato.shinichiro2@qst.go.jp, [e]makino.takahiro@qst.go.jp, [f]zkp@ansto.gov.au, [g]rns@ansto.gov.au, [h]luka.snoj@ijs.si, [i]vladimir.radulovic@ijs.si, [j]jose.coutinho@ua.pt, [k]vitor.torres@ua.pt, [l]k_demmouche@yahoo.fr

Keywords: 4*H*-SiC, deep level defects, neutrons, ion implantation, DLTS, carbon vacancy

We present a study of electrically active radiation-induced defects formed in 4*H*-SiC epitaxial layers following irradiation with fast neutrons, as well as 600 keV H^+ and 2 MeV He^{++} ion implantations. We also look at electron emission energies and mechanisms of the carbon vacancy in 4*H*-SiC by means of first-principles modelling. Combining the relative stability of carbon vacancies at different sites with the relative amplitude of the observed Laplace-DLTS peaks, we were able to connect Z_1 and Z_2 to emissions from double negatively charged carbon vacancies located at the *h*- and *k*-sites, respectively.

Introduction

Deep level defects that act as charge carrier traps have high importance in semiconductor industry and applications of semiconductor devices. These defects are mainly created during i) semiconductor material growth, ii) processing by ion implantation or iii) operation under harsh ionizing radiation conditions. In this work, we focus our attention on electrically active defects created in N-doped epitaxial 4*H*-SiC epitaxial layers exposed to irradiation by fast reactor neutrons, H^+ and He^{++} ion implants. We also investigate the acceptor levels of the carbon vacancy (V_C) by means of hybrid density functional supercell calculations.

Methods

n-type SiC Schottky barrier diodes (SBDs) were produced on nitrogen-doped (up to 5×10^{14} cm^{-3}) epitaxial grown 4*H*-SiC single crystal layers approximately 25 m thick [1]. The Schottky barrier was formed by evaporation of nickel through a metal mask with patterned square apertures of 1 mm × 1 mm, while Ohmic contacts were formed on the back side of the SiC substrate by nickel sintering at 950 °C in Ar atmosphere.

Samples were irradiated inside Cd thermal neutron filters with a wall thickness of 1 mm in the Pneumatic Tube (F24) irradiation location in the 250 kW JSI TRIGA reactor in Ljubljana. The neutron spectrum in the irradiation location was characterized previously on the basis of Monte Carlo calculations with the MCNP code and activation measurements [2,3]. The sub-cadmium flux was obtained from the characterized neutron spectrum and the Cd cutoff energy for the thickness of 1 mm, i.e. 0.55 eV.

Selected samples were implanted with 2 MeV He^{++} or 600 keV H^+ ions at the ANSTO nuclear microprobe facility [4]. Further implantation details can be found elsewhere [5].

The quality of SBD's was investigated by temperature dependent current-voltage (*I*-*V*) and capacitance-voltage (*C*-*V*) measurements. Deep level defects were analyzed by means of Deep Level Transient Spectroscopy (DLTS) and high-resolution Laplace-DLTS.

Density functional calculations were carried out using the VASP package [6]. We employed the projector-augment wave method to describe the core electrons [7], while a planewave basis with kinetic energy up to 400 eV was used to describe the valence. The exchange-correlation potential was evaluated using the hybrid density functional of Heyd-Scuseria-Ernzerhof (HSE06) [8].

Vacancy defects were inserted in 576-atom supercells, corresponding to 6×6×2 unit cells of 4*H*-SiC with lattice parameters a=3.071 Å and c=10.052 Å, and the Brillouin zone was sampled at **k**=(0 0 1/2). Energy levels were obtained by calculating the electron affinity of defective supercells with respect to the same quantity for a bulk supercell. The latter quantity is representative of the conduction band minimum energy. Total energies of charged supercells were adjusted by a periodic charge correction as proposed by Freysoldt, Neugebauer and Van de Walle [9].

Results and Discussion

DLTS spectra for the as-grown sample, as well as for selected irradiated and implanted samples are shown in Fig. 1. In the as-grown sample, only one peak is observed. The estimated activation energy for electron emission was 0.64 eV. This defect, known as $Z_{1/2}$ [10], has been reported as being the most dominant defect observed in as-grown 4*H*-SiC, and was ascribed to the V_C(=/0) transition.

From the first-principles calculations we found that neutral and double negative V_C defects show monoclinic structures which are labeled B and D, respectively. These possess

respectively 2 and 3 Si-Si distances distinctively shorter than the undistorted vacancy. Such short distances are identified as thick lines in Fig 2(a). We also found that the carbon vacancy in the negative charge state has two low-energy structures, namely C and D. While C is metastable by 0.03 eV in site-*k*, it is also the ground state in site-*h* (0.14 eV below structure D). These structures have been anticipated previously [11, 12]. From total energies and electron affinity calculations, we obtained the configurational coordinate diagram shown in Fig. 2(b). The lower energy states, namely $V_C^{\square}$ (D), are the most stable in n-type equilibrium conditions, i.e. after a zero-bias filling pulse in a DLTS experiment. When reverse bias is applied *T*~280-300 K, $V_C^{\square}$ defects within the depletion region become unstable against electron emission to the conduction band. The binding energy of this first emission is calculated as 0.64 eV, and the defect becomes singly negative. This figure matches the measured activation energy of $Z_{1/2}$ in the as-grown samples (Fig. 1). Structure D is still the most stable configuration for $V_C^{\square}(k)$. The binding energy for the second emission is now 0.61 eV only. This results from the strong relaxation towards structure B after the second emission. Hence, after the first emission, a second emission will follow immediately. Such a consecutive two-emission process is a fingerprint of a negative-*U* defect.

Regarding the *h*-site, the calculations indicate that like in the *k*-site, the first emission has a binding energy of 0.64 eV. However, it now involves a conversion between structures D and C.

For the neutron fluence of 10^{13} cm^{-2} the intensity of $Z_{1/2}$ related peak slightly increased, and an additional broad peak (ET2) with activation energy of 0.77 eV was observed (Fig. 1). Implantations of H^+ or He^{++} ions also lead to the increase $Z_{1/2}$ and to the introduction of an additional peak (ET1) shown in Fig. 1. The $Z_{1/2}$ related peak is broad with its peak maximum being shifted to higher temperatures with increasing fluences. A similar shift was already observed in 4*H*-SiC epi-layers irradiated with protons, alpha particles and electrons, and it was interpreted as the release of stress produced by defect clusters [5]. Notably, the shift was less pronounced in samples that were subject to annealing upon irradiation. Such treatments were not carried out in the present work. Estimated activation energies for electron emission from the irradiated samples are 0.68 and 0.71 eV for ET1 and $Z_{1/2}$, respectively. ET1 and ET2 traps were previously reported in the literature and were assigned to several defects [13,14]. Their low thermal stability is the only consensual property among the earlier studies. ET1 and ET2 traps might be simple defects with low thermal stability such as interstitials and Frenkel pairs, since they are introduced by different radiation sources and disappear after DLTS measurements up to 700 K [15].

We have performed preliminary L-DLTS measurements to obtain additional information about $Z_{1/2}$ and radiation introduced defects. Fig. 3 shows the Laplace spectra from the as-grown sample, as well as for the He-implanted sample measured at 292 K. The spectrum from the as-grown material indicates the presence of two peaks (two emission lines) instead of the single peak ($Z_{1/2}$) observed by conventional DLTS. In line with Ref. [13], the peak with lower emission rate is assigned to Z_2. The peak shows a higher amplitude compared to the one with higher emission rate, which is assigned to Z_1. We note that the observed L-DLTS peaks are unusually broad. By monitoring the change of the peak positions (and shape) over a wide range of temperature, we have eliminated the possibility that those peaks being an artefact from the measurement.

While electron paramagnetic resonance experiments were successful in distinguishing V_C defects in *k*- and *h*-sites [10] that has not been the case with conventional DLTS. Our calculations indicate that $V_C(k)$ is more stable than $V_C(h)$, irrespectively of the charge state and sub-lattice site. This suggests that the amplitude of Z_1 is lower than Z_2 in the L-DLTS spectrum of as-grown sample (see Fig. 3), simply because Z_2 arises from a defect that is more stable than Z_1. This allows us to connect Z_1 and Z_2 to $V_C(h)$ and $V_C(k)$, respectively.

The Laplace spectrum for the He^{++} implanted sample exhibits four emission lines (Fig. 3), among them are Z_1, Z_2 and ET1 related peaks. Unfortunately, due to peak overlap over a wide temperature range, we were not able to come up with a firm identification. However, the obtained result suggests that ET1 is not a simple defect. Further studies are needed to clarify this aspect.

Conclusions

We studied electrically active defects in the as-grown, fast-neutron irradiated and ion-implanted
4*H*-SiC epitaxial layers (25□m). The implants included 600 keV H^+ and 2 MeV He^{++} ions and the measurements were carried out by DLTS and L-DLTS. In addition, electron emission energies and mechanisms of the V_C in 4*H*-SiC by means of first-principles modelling were presented. We were able to separate emissions from Z_1 and Z_2 defects and connect them to double negatively charged V_C located at the *h*- and *k*-sites, respectively.

References

[1] M. Ito, L. Storasta, and H. Tsuchida, Appl. Phys. Express. 1, (2008) 015001-3.

[2] Snoj, L. et al., Computational analysis of irradiation facilities at the JSI TRIGA reactor, Applied Radiation and Isotopes, Volume 70, Issue 3, 2012, Pages 483-488.

[3] Trkov, A. et al., The GRUPINT neutron spectrum adjustment code – general features and characterization of the spectra in three irradiation channels of the JSI TRIGA reactor, International Symposium on Reactor Dosimetry (ISRD-16), 2017, May 7-12, Santa Fe (NM), USA.

[4] Z. Pastuovic, R. Siegele, D. D. Cohen, M. Ionescu, M. Mann, D. Button, S. Long, Nucl. Instr. Meth. Phys. Res. B 404, (2017) 1-8.

[5] Z.Pastuovic, I.Capan, D.D.Cohen, J.Forneris, N. Iwamoto, T.Ohshima, R.Siegele, N.Hoshino, and H.Tsuchida, Nucl. Inst. Meth. Phys. Res. B 348 (2015) 233-239.

[6] G. Kresse and J. Furthmüller, Phys. Rev. B 54 (1996) 11169.

[7] P. E. Blöchl, Phys. Rev. B 50 (1994) 17953.

[8] A. V. Krukau, O. A. Vydrov, A. F. Izmaylov, and G. E. Scuseria, J. Chem. Phys. 125 (2006) 224106.

[9] C. Freysoldt, J. Neugebauer, and C. G. Van de Walle, Phys. Rev. Lett. 102 (2009) 016402.

[10] N. T. Son, X. T. Trinh, L. S. Løvlie, B. G. Svensson, K. Kawahara, J. Suda, T. Kimoto, T. Umeda, J. Isoya, T. Makino, T. Ohshima, and E. Janzén, Phys. Rev. Lett. 109 (2012) 187603-5.

[11] X. T. Trinh, K. Szász, T. Hornos, K. Kawahara, J. Suda, T. Kimoto, A. Gali, E. Janzén, and N. T. Son, Phys. Rev. B 88 (2013) 235209.

[12] M. Bockstedte, A. Marini, O. Pankratov, and A. Rubio, Phys. Rev. Lett. 105 (2010) 026401.

[13] C. Hemmingsson, N. T. Son, O. Kordina, J. P. Bergman, E. Janzén, J. L. Lindström, S. Savage and N. Nordell, J. Appl. Phys. 81 (1997) 6155-6159.

[14] A. Castaldini, A. Cavallini, L. Rigutti, F. Nava, Appl. Phys. Lett. 85 (2004) 3780-3782.

[15]. Z. Pastuovic, I.Capan, S. Sato, T. Brodar, T. Ohshima, R. Siegele, submitted to J. Phys.: Condens. Matter

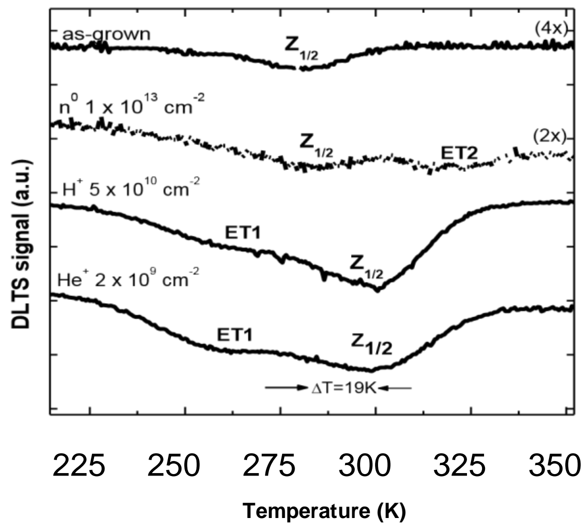

Fig. 1. DLTS spectra for the as-grown, fast neutron irradiated, 600 keV H^+ and 2 MeV He^{++} implanted samples. Fluences are given in the figure. The spectra were magnified and shifted vertically for clarity. Measurement settings were V_R=−10 V, V_P=−0.1 V, t_p=10 ms, time window is 100 ms.

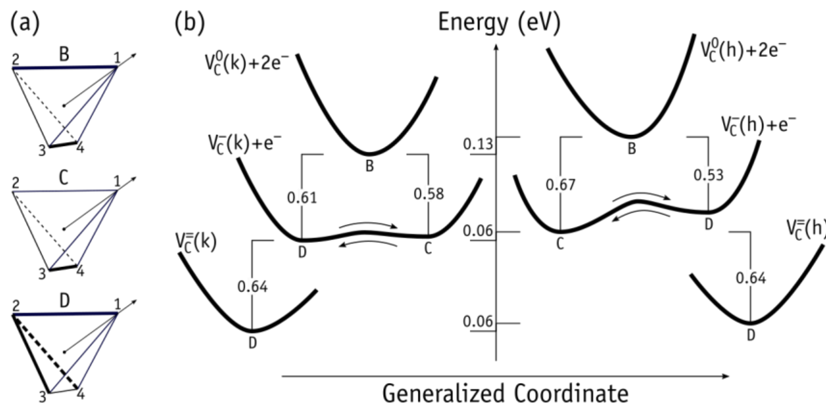

Fig. 2 (a) Diagrams of vacancy structures B, C and D. Shorter Si_i-Si_j distances ($1<i,j<4$) are shown as thick likes. The arrow is parallel to the *c*-axis. (b) Configuration coordinate diagram of $V_C(k)$ and $V_C(h)$ defects in n-type *4H*-SiC. Energy difference between ground states in each sub-lattice site are shown on the energy axis (energies are in eV).

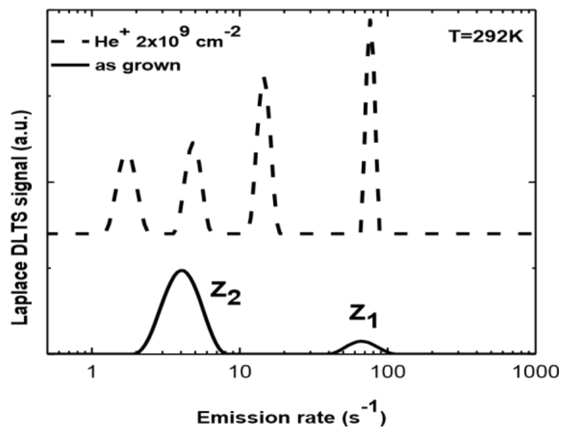

Fig.3 L-DLTS spectra for the as-grown (solid line) and He implanted sample (dash line) measured at 292 K. Voltage settings are the same as for DLTS (Fig.1).